

# Edge states and spin-valley edge photocurrent in transition metal dichalcogenide monolayers

V.V. Enaldiev<sup>1,\*</sup>

<sup>1</sup>*Kotel'nikov Institute of Radio-engineering and Electronics of the Russian Academy of Sciences, 11-7 Mokhovaya St, Moscow, 125009 Russia*

(Dated: December 14, 2024)

We develop an analytical theory for edge states in monolayers of transition metal dichalcogenides based on a general boundary condition for a two-band **kp**-Hamiltonian in case of uncoupled valleys. Taking into account *edge* spin-orbit interaction we reveal that edge states, in general, have linear dispersion that is determined by three real phenomenological parameters in the boundary condition. In absence of the spin-orbit interaction, edge states are described by a single real parameter whose sign determines whether their spectra intersect the gap or not. In the former case we show that illumination by circularly polarised light results in spin and valley polarised photocurrent along the edge. Flow direction, spin and valley polarisation of the edge photocurrent are determined by the direction of circular polarisation of the illuminated light.

## I. INTRODUCTION

The optical properties of monolayer crystals of transition metal dichalcogenides (TMDs) (like MoS<sub>2</sub>, MoSe<sub>2</sub>, MoTe<sub>2</sub>, WS<sub>2</sub>, and WSe<sub>2</sub>) have recently attracted a considerable interest due to possible optoelectronic applications<sup>1,2</sup>. This is due to the direct band gap of the TMD monolayers whose value corresponds to the visible and infrared light frequencies<sup>3</sup>. The optical response of the bulk materials at absorption edge is dominated by excitons<sup>4</sup>. However, recent experiments on second harmonic generation at sub-band gap frequencies<sup>5</sup>, scanning tunneling microscopy and spectroscopy<sup>6,7</sup> as well as microwave impedance microscopy<sup>8</sup> in MoS<sub>2</sub>-monolayers have also exhibited edge state (ES) signs.

From theoretical point of view properties of ESs in atomically thin MoS<sub>2</sub> are extensively studied in frames of density functional theory<sup>7,9-13</sup> as well as tight-binding approximation<sup>14,15</sup>. However description of the ESs in the TMD monolayers within **kp**-approach allows one to describe the ESs without going into details of edge microscopic structure and to take into account effects of external fields. This enables to construct an analytic theory for the ESs in the whole class of materials in a unified way. Such a general theory relies on a boundary condition (BC) that describes the edge structure by means of several phenomenological parameters. The values of these parameters can be obtained by fitting with experimental data or other calculations based on density-functional or tight-binding approximations. Authors of Ref.[16] derive a general boundary condition taking into account valley coupling at the edge and neglecting by edge spin-orbit interaction which may, in general, exist (see Ref.[17] and references therein). Recently, ES spectra in the TMD monolayer nanoribbon<sup>18</sup> and optical absorption in TMD nanoflakes involving transitions between the bulk and edge states<sup>19</sup> have been studied in the **kp**-approximation. However, these studies were restricted by some certain values of the phenomenological boundary parameters.

The aim of this paper is twofold. First, we develop an analytical theory for the ESs in the TMD monolayers in the **kp**-approach taking into account edge spin-orbit interaction in the case of uncoupled valleys. Second, we consider optoelectronic properties of the ESs and demonstrate an emergence of spin and valley polarised edge photocurrents due to illumination of the monolayer by circularly polarised light. Origin of the effect is similar with valley Hall effect<sup>20</sup> and concerns with selection rules for circularly polarised light in the two valleys. The paper is organized as follows: in Sec.II we derive a general boundary condition and resulting ES spectra for two-band continuum model, Sec.III is devoted to derivation of the edge photocurrent.

## II. EDGE STATES IN TWO-BAND KP-APPROXIMATION

In the TMD monolayers conduction and valence band edges are located in  $K$  and  $K'$  valleys of the honeycomb lattice Brillouin zone. Within a two-band **kp**-approach, dynamics of electrons with spin  $s/2 = \pm 1/2$  in the  $K$  ( $K'$ ) valley is described by the Hamiltonian<sup>3,21</sup>

$$H_\tau = \begin{pmatrix} m + \tau\Delta_c & v(\tau p_x - ip_y) & 0 & 0 \\ v(\tau p_x + ip_y) & -m + \tau\Delta_v & 0 & 0 \\ 0 & 0 & m - \tau\Delta_c & v(\tau p_x - ip_y) \\ 0 & 0 & v(\tau p_x + ip_y) & -m - \tau\Delta_v \end{pmatrix} \quad (1)$$

where  $2m$  is the band gap without spin splitting,  $2\Delta_{c,v}$  is the value of spin splitting in the conduction and valence band correspondingly, the index  $\tau = +1(-1)$  denotes the  $K$  ( $K'$ ) valley,  $\mathbf{p} = (p_x, p_y)$  is the in-plane 2D momentum,  $v$  is the velocity matrix element between the band extrema. The Hamiltonian  $H_\tau$  (1) possesses diagonal form in the spin subspace. To describe edge of the TMD monolayer one should supplement the Hamiltonian with a BC for envelope wave functions. In present work

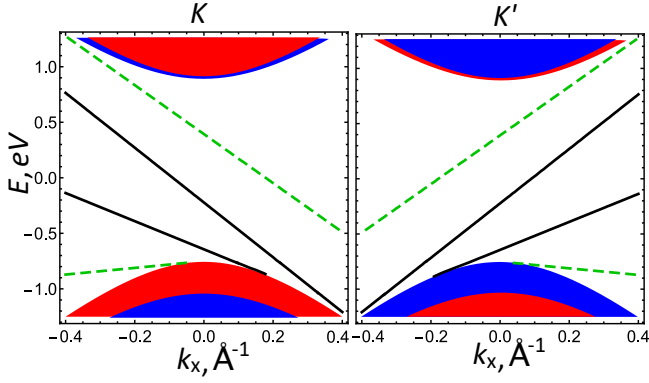


FIG. 1. Spectra of edge states in K valley (left) and K' valley (right) derived from Eq. (6) with the following phenomenological parameters: Dashed green lines respond to  $\xi = -2.9$ ,  $\eta = 0.5$ ,  $\nu = 0.6$ ; solid black lines respond to  $\xi = -2.9$ ,  $\eta = 1.5$ ,  $\nu = 0.6$ . Shaded regions shows projections of bulk bands. Bulk parameters are as follows:  $2m = 1.8$  eV,  $\Delta_c = 10$  meV,  $\Delta_v = 143$  meV,  $v = 2.5$  eV·Å.

we consider a translation invariant edge for which projections of the valley centers onto the edge direction are well distant from each other (like at zigzag or reconstructed zigzag edges). Therefore, we will neglect by the valley coupling at the edge.

However, even at the translation invariant edge, additional *edge* spin-orbit interaction can mix the spins<sup>17</sup>. In our theory this entanglement is described by a general BC that couples wave functions with definite spin projection:

$$[\Psi_\tau^\uparrow + M_\tau \Psi_\tau^\downarrow]_{\text{edge}} = 0 \quad (2)$$

where  $\Psi_\tau^{\uparrow(\downarrow)} = (\psi_{c,\tau}^{\uparrow(\downarrow)}, \psi_{v,\tau}^{\uparrow(\downarrow)})^T$  is two component wave function for spin up (down) states and  $M_\tau$  is the second order square matrix consisting of phenomenological parameters that characterize the edge structure. Explicit form of the matrix  $M_\tau$  is determined by the Hermiticity of the Hamiltonian  $H_\tau$ :

$$M_\tau^+ \mathbf{n} \sigma_\tau M_\tau + \mathbf{n} \sigma_\tau = 0 \quad (3)$$

where  $\sigma_\tau = (\tau\sigma_x, \sigma_y)$  is vector of Pauli matrix,  $\mathbf{n} = (n_x, n_y)$  is a unit outer normal to the edge. Time reversal symmetry relates the boundary matrices from the two valleys:  $M_\tau^{-1} = M_{-\tau}^*$ . These conditions lead us to the four-parametric form for matrix  $M_\tau$ :

$$M_\tau = e^{i\chi} \cos \xi \sinh \eta \times \begin{pmatrix} i \left( \frac{\tanh \xi}{\sinh \eta} + \tau \coth \eta \cos \nu \right) & e^{-i\tau\varphi} (1 - \coth \eta \sin \nu) \\ e^{i\tau\varphi} (1 + \coth \eta \sin \nu) & i \left( \frac{\tanh \xi}{\sinh \eta} - \tau \cosh \eta \cos \nu \right) \end{pmatrix}, \quad (4)$$

where  $e^{\pm i\tau\varphi} = n_x \pm \tau i n_y$ ,  $\chi, \xi, \eta, \nu$  ( $0 \leq \chi, \nu < 2\pi$ ,  $-\infty < \xi, \eta < +\infty$ ) are the real phenomenological parameters characterizing edge properties. The edge spin-orbit

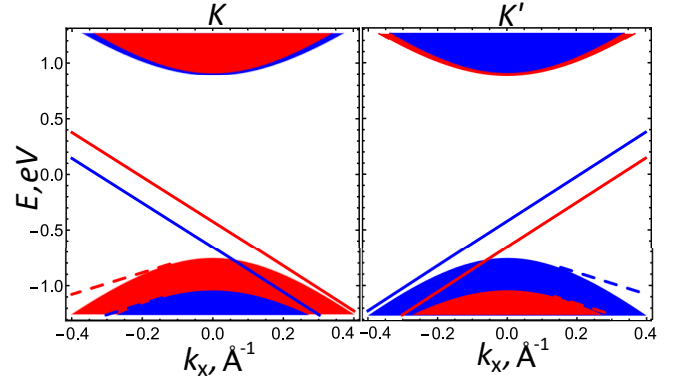


FIG. 2. Spectra of spin-polarised edge states (7) in absence of spin-orbit interaction (i.e.  $a_{+1,\tau} = a_{-1,\tau}$ ) in K valley (left) and K' valley (right). Solid lines respond to  $a_{\pm 1,\tau} = 0.5$ ; dashed lines respond to  $a_{\pm 1,\tau} = -0.2$ . Shaded regions shows projections of bulk bands. Bulk parameters are the same as on Fig. 1.

interaction is described by the parameters  $\xi$ ,  $\eta$  and  $\chi$ , but  $\nu$  is responsible for mixing of wave functions of conduction and valence bands with the same spin. Now we are able to calculate spectra of ESs with the general BC (2),(4). Suppose that the 2D crystal fills a half-plane  $y > 0$ . Then, ES wave function is of the form:

$$\Psi_\tau^{\uparrow(\downarrow)} = C_\tau^{\uparrow(\downarrow)} \left( \frac{1}{\hbar v (\tau k_x - \kappa_\tau^{\uparrow(\downarrow)})} \right) e^{-\kappa_\tau^{\uparrow(\downarrow)} y + i k_x x} \quad (5)$$

where  $s = +1 (-1)$  for states with spin  $\uparrow (\downarrow)$ ,  $C_\tau^{\uparrow(\downarrow)}$  is a normalization constant,  $\kappa_\tau^{\uparrow(\downarrow)} = \{k_x^2 - (\varepsilon - m + s\tau\Delta_c)(\varepsilon + m - s\tau\Delta_v)/(\hbar v)^2\}^{1/2}$  is a decay length of ESs. Substituting wave function (5) in the BC (2) we obtain a general dispersion equation for ESs:

$$\left[ \varepsilon + m - \tau\Delta_v + \tau\hbar v (\tau k_x - \kappa_\tau^\uparrow) \frac{1 + \tau \cosh \eta \cos \nu}{\sinh \eta + \cosh \eta \sin \nu} \right] \times \left[ \varepsilon + m + \tau\Delta_v - \tau\hbar v (\tau k_x - \kappa_\tau^\downarrow) \frac{1 - \tau \cosh \eta \cos \nu}{\sinh \eta + \cosh \eta \sin \nu} \right] + \frac{\tau v (\tanh \xi - 1)}{\sinh \eta + \cosh \eta \sin \nu} \left[ (\tau k_x - \kappa_\tau^\uparrow) (\varepsilon + m + \tau\Delta_v) - (\tau k_x - \kappa_\tau^\downarrow) (\varepsilon + m - \tau\Delta_v) \right] = 0. \quad (6)$$

On Fig.1 we reveal typical dispersion of ESs in the K and K' valleys given by the previous equation. We note that Eq.(6) and, consequently, ES spectra do not depend on the value of parameter  $\chi$ . In general case ESs exist for those longitudinal momenta when their energies are not overlapped with projections of bulk bands. From Eq.(6) it follows that two spin components are unraveled in the limit  $\xi \rightarrow +\infty$ . Although this does not mean vanishing of the edge spin-orbit interaction as ES spectra for each spin projection will be determined by its own single parameter

$$a_{s,\tau} = s\tau(1 + s\tau \cosh \eta \cos \nu)(\sinh \eta + \cosh \eta \sin \nu):$$

$$\varepsilon_e^{\uparrow(\downarrow)}(p_x) = -\frac{2a_{s,\tau}}{1 + a_{s,\tau}^2} \tau v p_x - \frac{1 - a_{s,\tau}^2}{1 + a_{s,\tau}^2} m + \frac{s\tau(\Delta_v + a_{s,\tau}^2 \Delta_c)}{1 + a_{s,\tau}^2}, \quad (7)$$

Valley index  $\tau$  determines chirality of ESs (see Fig. 2) which exist for those wave vectors  $k_x$  while their decay length is positive:

$$\kappa_\tau^{\uparrow(\downarrow)} = -\tau \kappa_x \frac{1 - a_{s,\tau}^2}{1 + a_{s,\tau}^2} + \frac{2a_{s,\tau}}{1 + a_{s,\tau}^2} \frac{\tilde{m}_{s,\tau}}{\hbar v} > 0. \quad (8)$$

here  $\tilde{m}_{s,\tau} = m - s\tau(\Delta_v - \Delta_c)/2$ . We note that condition (8) allows spin-polarised ESs to exist even when their spectra are overlapped with projection of bulk band characterized by opposite spin. In particular, inequality (8) specifies that at  $a_{s,\tau} > 0$  ES spectra intersect the bulk gap, but at  $a_{s,\tau} < 0$  they are out of the gap (see Fig. 2). We note that  $a_{s,\tau} = a_{-s,-\tau}$ , which is a consequence of time reversal symmetry. In absence spin-orbit interaction at the edge ( $\eta \rightarrow +\infty$ )  $a_{\pm 1,\tau} = \cos \nu / (1 + \sin \nu)$ , ES spectra for two spins are parallel to each other with constant energy difference for every momenta:  $\varepsilon_e^\uparrow - \varepsilon_e^\downarrow = 2\tau(\Delta_v + a_{1,\tau}^2 \Delta_c) / (1 + a_{1,\tau}^2)$ . Under validity of spectra (7) wave function of ES is of the form:

$$\Psi_e^{\uparrow(\downarrow)} = C_\tau^{\uparrow(\downarrow)} \begin{pmatrix} 1 \\ -\frac{\tau}{a_{s,\tau}} \end{pmatrix} e^{-\kappa_\tau^{\uparrow(\downarrow)} y + i k_x x}, \quad (9)$$

where  $C_\tau^{\uparrow(\downarrow)} = \left[ 2a_{s,\tau}^2 \kappa_\tau^{\uparrow(\downarrow)} / L_x (1 + a_{s,\tau}^2) \right]^{1/2}$  is the normalization factor.

### III. SPIN-VALLEY EDGE PHOTOCURRENTS

In this section we reveal that illumination of semi-infinite 2D TMD crystal by circularly polarised light induces spin and valley polarised edge photocurrents. As we mentioned in introduction the effect is due to difference in transition probabilities between bulk and edge bands in the two valleys caused by the light.

For definiteness and simplicity we consider absence of spin-orbit interaction at the edge. Therefore ESs are described by a single parameter  $a$  for both spins and valleys (we suppressed spin and valley index). However, obtained results are also valid when the two spin-polarised ES branches are described by different parameters  $a_{+1,\tau} \neq a_{-1,\tau}$  (7), while one can populate only one of them in each valley. We will regard that  $a \sim 1$ , so that ES spectra intersect the gap as shown on Fig.3. This situation agrees with tight-binding calculations of ES spectra at zigzag edge of MoS<sub>2</sub><sup>15</sup>. Further throughout this section we suppress the valley index  $\tau$  everywhere except where it is needed.

Now we turn to the bulk states. Around the band extremum, energies of the spin up (down) states in valence

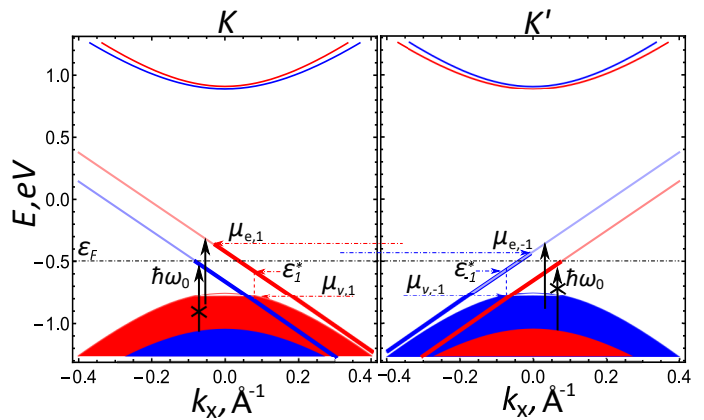


FIG. 3. Schematic picture of quasi Fermi-levels in edge ( $\mu_{e,\pm 1}$ ) and valence ( $\mu_{v,\pm 1}$ ) bands under illumination of clockwise circular polarised light with frequency  $\omega_0$  in case of spin polarised ESs described by the formula (7) with  $a_{+,\tau} = a_{-,\tau} > 0$ .  $\varepsilon_F$  is equilibrium Fermi-energy.  $\varepsilon_{\pm 1}^*$  is the minimal energy of ESs that radiatively recombine with holes in valence band.

band of  $K$  ( $K'$ ) valley are expressed as follows:

$$\varepsilon_v = \varepsilon_t - \frac{(vp)^2}{2\tilde{m}}, \quad (10)$$

where  $\varepsilon_t = -m + \Delta_v$  is energy of the upper valence band top in each valley,  $p = \sqrt{p_x^2 + p_y^2}$  is 2D momentum modulus. For the type of edge under consideration, bulk states should satisfy a single parameter BC:  $[\psi_c + a\psi_v]_{y=0} = 0$ , which is obtained from the BC (2) in the limit  $\xi, \eta \rightarrow +\infty$ . This BC is satisfied by superposition of incident and scattered off the edge plane waves with a common longitudinal momentum  $p_x$ :

$$\Psi_{p_x, \varepsilon_v} = \frac{1}{\sqrt{2}} [\psi_{p_x, -p_y} + R_{\varepsilon_v, k_x} \psi_{p_x, p_y}] \quad (11)$$

where  $\psi_{p_x, \pm p_y}$  are plane wave solutions of the Hamiltonian (1),  $R_{\varepsilon_v, k_x}$  is a reflection coefficient that is determined by the BC. Plane wave states around extrema of valence band are of the form:

$$\psi_{p_x, p_y} = \frac{1}{\sqrt{L_x L_y}} \begin{pmatrix} -\frac{vp}{2\tilde{m}} \\ e^{i\vartheta_p} \end{pmatrix} e^{i\mathbf{k}\mathbf{r}}, \quad (12)$$

where  $L_x L_y$  is the system area,  $e^{i\vartheta_p} = (\tau p_x + i p_y) / p$ ,  $\mathbf{k} = \mathbf{p} / \hbar$  is 2D wave vector. In fact in semi-infinite sample  $p_y$  is not a good quantum number and should be treated as a function of energy and  $p_x$  from Eq. (10):  $p_y(\varepsilon, p_x) = [\sqrt{2\tilde{m}/v}] \sqrt{\varepsilon_t - \varepsilon_v - (vp_x)^2 / 2\tilde{m}}$ . For valence band states with energies around band extrema reflection coefficient can be approximated as follows  $R_{\varepsilon_v, k_x} \approx -e^{-i2\theta_p}$ .

We suppose that the semi-infinite 2D crystal is illuminated in negative direction of  $z$ -axis by a clockwise polarised light with frequency  $\omega_0$  (in case of counter clockwise polarisation one should exchange  $\tau \rightarrow -\tau$  in final

formulae (18),(19)). Due to spin splitting of the valence bands (order of 0.1 eV) one can tune frequency  $\omega_0$  of illuminated light and Fermi-energy  $\varepsilon_F$  in the monolayer, to induce electrical dipole transitions only from the up valence band in the  $K$  ( $K'$ ) valley to ESs with the corresponding spin (see Fig.3). Our aim is to calculate induced edge photocurrent owing to these transitions. To this end we derive kinetic equation for distribution function in frames of Keldysh formalism<sup>22</sup> (see Appendix A):

$$\begin{aligned} \frac{\partial f_e(\varepsilon)}{\partial t} &= W_{\varepsilon-\hbar\omega_0,\varepsilon}^{ind} [f_v(\varepsilon - \hbar\omega_0) - f_e(\varepsilon)] - \\ f_e(\varepsilon) \int_0^{+\infty} W_{\varepsilon-\hbar\omega,\varepsilon}^{sp} [1 - f_v(\varepsilon - \hbar\omega)] d\omega &- \frac{f_e(\varepsilon) - f_{eq}(\varepsilon)}{\tau_R}, \end{aligned} \quad (13)$$

where  $f_{e,v}(\varepsilon)$  is Fermi-Dirac distribution function for states in edge/valence band respectively,  $f_{eq}(\varepsilon)$  is equilibrium Fermi-Dirac function,  $W_{\varepsilon-\hbar\omega_0,\varepsilon}^{ind}$  is a rate of induced transitions between edge state, characterized by longitudinal momentum  $p_e$  and energy  $\varepsilon$ , and the valence band state with the same longitudinal momentum and energy  $\varepsilon - \hbar\omega$ ,  $W_{\varepsilon-\hbar\omega,\varepsilon}^{sp} d\omega$  is a rate of spontaneous transitions caused by interaction with ground state of electromagnetic field,  $\tau_R$  is a phenomenological relaxation time that describes other relaxation processes between edge and valence band states caused by, for example, phonon or electron-electron scattering (below we discuss range of the relaxation time). The rate of the induced transitions reads as follows

$$W_{\varepsilon-\hbar\omega_0,\varepsilon}^{ind} = \frac{2\pi}{\hbar} \frac{I\Omega}{c\hbar\omega_0} \left| V_{\varepsilon-\hbar\omega_0,\varepsilon}^{(+,\tau)}(\mathbf{q}_0) \right|^2 \rho_{v,e}(\varepsilon - \hbar\omega_0) \quad (14)$$

where  $I$  is intensity of the incident light,  $c$  is the speed of light,  $\Omega$  is a volume for quantization of electromagnetic field,  $V_{\varepsilon-\hbar\omega_0,\varepsilon}^{(+,\tau)}(\mathbf{q}_0)$  is the matrix element of interaction between valence and edge band states (A4), density of the valence band states with definite longitudinal momentum  $p_e$  near valence band extrema is expressed by the formula:

$$\rho_{v,e}(\varepsilon) = \sum_{p_y} \delta(\varepsilon - \varepsilon_{p_e,p_y}) = \frac{L_y \sqrt{2\tilde{m}}}{2\pi\hbar v} \frac{\Theta\left(\varepsilon_t - \frac{v^2 p_e^2}{2\tilde{m}} - \varepsilon\right)}{\sqrt{\varepsilon_t - \frac{v^2 p_e^2}{2\tilde{m}} - \varepsilon}}, \quad (15)$$

where  $\Theta(\dots)$  is the Heaviside step function. The probability of spontaneous transitions is expressed as follows:

$$W_{\varepsilon-\hbar\omega,\varepsilon}^{sp} = \frac{\Omega}{(2\pi)^2 \hbar c^3} \sum_{\lambda=\pm} \int d\omega_q \left| V_{\varepsilon-\hbar\omega,\varepsilon}^{(\lambda,\tau)}(\mathbf{q}) \right|^2 \rho_{v,e}(\varepsilon - \hbar\omega), \quad (16)$$

here integration goes over solid angle of light wave vector  $\mathbf{q}$ , summation runs over clockwise ( $\lambda = +$ ) and counter

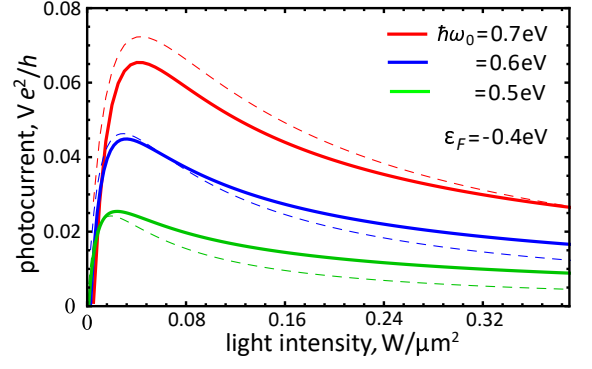


FIG. 4. Dependence of photocurrent (20) on intensity of illuminating light at three different frequencies  $\hbar\omega_0 = 0.7$  eV (red),  $\hbar\omega_0 = 0.6$  eV (blue) and  $\hbar\omega_0 = 0.5$  eV (green). Solid lines represent solution for quasi Fermi-levels derived from Eq.(B2). Dashed lines correspond to the approximated solution (19). Equilibrium Fermi-energy is  $\varepsilon_F = -0.4$  eV. Bulk parameters are similar to Fig.1, boundary parameter  $a = 0.8$ . Phenomenological relaxation time  $\tau_R = 1$  ns, length characterizing the TMD monolayer in perpendicular to the edge direction is  $L_y = 1 \mu m$ .

clockwise ( $\lambda = -$ ) polarisation of the electromagnetic field.

It is known that intraband energy relaxation processes have the shortest times in MoS<sub>2</sub> monolayers<sup>23,24</sup> (order of picoseconds). As electron-electron scattering is very efficient in one dimension channel we suppose that relaxation within the edge band is of the same order. This allows us to solve the kinetic equation (13) in quasi-equilibrium approximation, which is justified when intraband relaxation times is shorter than edge-bulk energy relaxation times. Therefore, we look for distribution function of the edge (valence) states in the form of Fermi-Dirac function with its own quasi Fermi-level  $\mu_{e,\tau}$  ( $\mu_{v,\tau}$ ). We also suppose that additional edge-to-valence band energy relaxation processes, characterized by the relaxation time  $\tau_R$  order of nanoseconds. This is mainly due to suppression of phase-space for these processes caused by great difference in density of bulk and edge states. This allows edge-to-valence scattering only with certain longitudinal momentum mismatch (as valence band quasi Fermi-level locates around the top of valence band).

We are interested in stationary solution that equates the right-hand side of Eq.(13) to zero. After integration the kinetic equation over energy in the limit of zero temperature we arrive to the first implicit relation for  $\mu_{e,\tau}$  and  $\mu_{v,\tau}$  (B2). Another relation between quasi Fermi-levels is imposed by a particle conservation rule (i.e. the number of holes in the valence band equals the number of photo-excited electrons in the edge band):

$$(\varepsilon_t - \mu_{v,\tau}) \rho_v = (\mu_{e,\tau} - \varepsilon_F) \rho_e \quad (17)$$

where  $\rho_v = L_y L_x \tilde{m} / 2\pi (\hbar v)^2$  is density of states in valence band,  $\rho_e = L_x (1 + a^2) / 2\pi \hbar v 2|a|$  is density of edge states. By virtue of ratio between the densities  $\rho_e / \rho_v \propto$

$\hbar v/\tilde{m}L_y \ll 1$  one has inequality  $|\varepsilon_v - \mu_{v,\tau}| \ll |\mu_{e,\tau} - \varepsilon_F|$ , which leads us to a simpler equation for  $\mu_{e,\tau}$  (in comparison with Eq.(B2)):

$$\frac{I}{I_0} \left\{ \delta_{\tau,1} + \delta_{\tau,-1} \left( \frac{\hbar v \kappa_F}{2\tilde{m}a} \right)^2 \right\} \times \left[ \arctan \left( \frac{k_{y0}(\mu_{e,\tau} - \hbar\omega_0)}{\kappa_F} \right) - \frac{\kappa_F k_{y0}(\mu_{e,\tau} - \hbar\omega_0)}{\kappa_F^2 + k_{y0}^2(\mu_{e,\tau} - \hbar\omega_0)} \right] - \frac{\mu_{e,\tau} - \varepsilon_F}{\hbar\omega_0^2 \tilde{\tau}_R} = 0, \quad (18)$$

here  $I_0 = \hbar\omega_0^4/c^2$ ,  $\tilde{\tau}_R = \tau_R [(v/c)^2(e^2/\hbar c)4\pi a^2/(1+a^2)n_\tau^2]$ ,  $k_{y0}(\mu_{e,\tau} - \hbar\omega_0) = p_y(\mu_{e,\tau} - \hbar\omega_0, p_x = 0)/\hbar$ . Deriving Eq.(18) we neglected by the dependence of decay length of ESs on the energy (i.e.  $\kappa(\varepsilon) \approx \kappa(\varepsilon_F) \equiv \kappa_F$ ) and  $p_y(\varepsilon, p_e)$  on  $p_e$ , as we consider the valence band states around band extrema with momenta  $vp \ll 2\tilde{m}$ . It is the expression in the curly brackets of Eq.(18) that describes difference in edge band population in the  $K$  and  $K'$  valleys. This results in uncompensated edge photocurrent with certain spin in particular valley. In the limit  $\mu_{e,\tau}/\varepsilon_F \ll 1$  we obtain explicit expression for electron quasi Fermi-level in the edge band:

$$\mu_{e,\tau} = \varepsilon_F + \frac{\frac{I}{I_0} \hbar\omega_0^2 \tilde{\tau}_R G(\varepsilon_F - \omega_0) \left\{ \delta_{\tau,1} + \delta_{\tau,-1} \left( \frac{\hbar v \kappa_F}{2\tilde{m}a} \right)^2 \right\}}{1 + \frac{I}{I_0} \frac{2\tilde{m}\hbar\omega_0^2 \tilde{\tau}_R}{(\hbar v)^2} \frac{\kappa_F k_{y0}(\varepsilon_F - \omega_0)}{[\kappa_F^2 + k_{y0}^2(\varepsilon_F - \omega_0)]^2} \left\{ \delta_{\tau,1} + \delta_{\tau,-1} \left( \frac{\hbar v \kappa_F}{2\tilde{m}a} \right)^2 \right\}}, \quad (19)$$

where

$$G(\varepsilon) = \arctan \left( \frac{k_{y0}(\varepsilon)}{\kappa_F} \right) - \frac{\kappa_F k_{y0}(\varepsilon)}{\kappa_F^2 + k_{y0}^2(\varepsilon)}.$$

With known quasi Fermi-levels of the ESs in the two valleys, we use a standard formula for one-dimensional current along the sample edge:

$$j = \frac{e}{h} (\mu_{e,1} - \mu_{e,-1}). \quad (20)$$

Dependence of the photocurrent on the light intensity is plotted on Fig.4. Solid lines show photocurrent obtained by solving Eq.(B2) for electron quasi Fermi-levels, dashed lines represent approximated solution (19). At small intensities, the current (20) is a linear function of the intensity with a tilt that are determined by the edge-valence band transition probability difference in the  $K$  and  $K'$  valleys. However, in the limit of high intensities the current goes to zero as edge bands in both valleys tend to equal population. It gives rise to a maximum photocurrent in middle region of intensities. Using solutions (19) one can obtain an approximated expression for maximal current in Fig.4:

$$j_{\max} = \frac{e^2}{h} (\varepsilon_t - \varepsilon_F + \omega_0) \frac{1 - \frac{\hbar v \kappa_F}{2\tilde{m}a}}{1 + \frac{\hbar v \kappa_F}{2\tilde{m}a}}, \quad (21)$$

which is valid in the limit  $k_{y0}(\varepsilon_F - \omega_0)/\kappa_F \ll 1$ . Therefore, the greater valence-to-edge transition probability difference in the two valleys, the higher maximal value of spin-valley polarised current along the edge. Absolute values of the maximal current can attain several microamperes. In case of clockwise polarization of light, uncompensated photocurrent flows in the  $K$  valley in negative direction along the edge (see Fig.3). As it was mentioned above for counter-clockwise polarisation one should exchange  $\tau \rightarrow -\tau$  in (19), which leads to uncompensated photocurrent in the  $K'$  valley but in positive direction along the edge. Thus, direction of light polarisation controls not only spin and valley polarisation of the uncompensated edge photocurrent but also its direction of flowing.

#### IV. CONCLUSION

We derived a theory of ESs in monolayers of TMD crystals which takes into account edge spin-orbital interaction within intra-valley approximation. The theory relies on the phenomenological boundary condition described, in general, by four real parameters that characterize edge structure. In general case ESs have linear spectra described by only three of the parameters, two of which are responsible for spin-orbit coupling but the remaining one for interband interaction with the same spin. In limiting case of chiral and spin-polarised ESs, their spectra are described by a single parameter for each spin whose sign determines whether their spectra are in the bulk gap or outside of the latter.

We also considered optical pumping from valence band to ESs in absence of the edge spin-orbit interaction and demonstrate a possibility for generation of spin and valley polarised edge photocurrents. We revealed that direction, valley and spin polarisation of the photocurrent is determined by direction of circular polarisation of the light. Maximal values of the photocurrent are order of several microamperes.

#### ACKNOWLEDGMENTS

This work was supported by the Russian Foundation for Basic Research (project 16-32-00655).

#### Appendix A: Derivation of kinetic equation (13)

In order to derive the kinetic equation (13) we first write down the Hamiltonian of the system under consid-

eration in terms of second-quantization operators:

$$H_0 = \sum_{p_e} \varepsilon_e a_{p_e}^+ a_{p_e} + \sum_{p_x, p_y} \varepsilon_{v, p_x, p_y} a_{v, p_x, p_y}^+ a_{v, p_x, p_y} + \sum_{p_x, p_y} \varepsilon_{c, p_x, p_y} a_{c, p_x, p_y}^+ a_{c, p_x, p_y} + \sum_{\mathbf{q}, \lambda = \pm} \hbar\omega \left( c_{\mathbf{q}, \lambda}^+ c_{\mathbf{q}, \lambda} + \frac{1}{2} \right), \quad (\text{A1})$$

where  $a_{p_e}$  ( $a_{p_e}^+$ ) is annihilation (creation) operator of the edge state (9) with energy  $\varepsilon_e$ ,  $a_{v/c, p_x, p_y}$  ( $a_{v/c, p_x, p_y}^+$ ) is annihilation (creation) operator of the valence/conduction band state (11) with energy  $\varepsilon_{v/c, p_x, p_y}$ ,  $c_{\mathbf{q}, \lambda}$  ( $c_{\mathbf{q}, \lambda}^+$ ) is annihilation (creation) operator of photon with clockwise ( $\lambda = +$ ) or counter-clockwise ( $\lambda = -$ ) polarisation and energy  $\omega = cq$ . In previous equation we suppress spin and valley indexes for brevity. In terms of the creation and annihilation operators of photon field vector-potential reads as follows:

$$\mathbf{A}(\mathbf{r}, t) = \sum_{\mathbf{q}, \lambda = \pm} \sqrt{\frac{2\pi c^2 \hbar}{n_r^2 \omega \Omega}} \left[ c_{\mathbf{q}, \lambda} \mathbf{e}_\lambda e^{i(\mathbf{q}\mathbf{r} - \omega t)} + c_{\mathbf{q}, \lambda}^+ \mathbf{e}_\lambda^* e^{-i(\mathbf{q}\mathbf{r} - \omega t)} \right], \quad (\text{A2})$$

where  $\Omega$  is quantization volume, polarisation unit vectors  $\mathbf{e}_{\mathbf{q}, \pm} = [1/\sqrt{2}] (\cos \alpha_q \pm i \sin \alpha_q \cos \theta_q, -\sin \alpha_q \pm i \cos \alpha_q \cos \theta_q, \mp i \sin \theta_q)$  (spherical angles  $\alpha_q, \theta_q$  characterize direction of the photon wave-vector  $\mathbf{q} = q (\sin \alpha_q \sin \theta_q, \cos \alpha_q \sin \theta_q, \cos \theta_q)$ ). Interaction of Dirac fermions with electromagnetic field reads as follows:

$$V_{int} = \sum_{p_e, p_x, p_y, \mathbf{q}, \lambda = \pm} \left[ V_{\varepsilon_v, \varepsilon_e}^{(\lambda, \tau)}(\mathbf{q}) a_{p_e}^+ c_{\mathbf{q}, \lambda} a_{v, p_x, p_y} + h.c. \right], \quad (\text{A3})$$

where we take into account only transitions between valence band electrons and edge states that are determined in dipole approximation by the matrix elements:

$$V_{\varepsilon_v, \varepsilon_e}^{(\lambda, \tau)}(\mathbf{q}) = \tau \delta_{p_e, p_x} \frac{ve}{c} \sqrt{\frac{2\pi c^2 \hbar}{n_r^2 \omega \Omega}} \frac{C_e \sqrt{L_x}}{\sqrt{2L_y}} \frac{2ik_y(\varepsilon, p_e)}{\kappa^2 + k_y^2(\varepsilon, p_e)} \times \left[ \frac{e^{-i\tau\alpha_q}}{\sqrt{2}} (1 + \tau\lambda \cos \theta_q) + \frac{e^{i\tau\alpha_q}}{\sqrt{2}} (1 - \tau\lambda \cos \theta_q) \frac{\hbar v \kappa + \tau v p_e}{2\tilde{m}a} \right] \quad (\text{A4})$$

From the previous formula it follows that ratio of probabilities for induced transitions (at normal incidence of light  $\cos \theta_q = 1$ ) in the two valleys for definite polarisation has an order of  $(\hbar v \kappa / 2\tilde{m}a)^2 \approx 1/4 \ll 1$  at the boundary parameter values  $|a| \approx 1$ .

Now we introduce Keldysh Green functions of DFs  $G_\nu^{\alpha\beta}(t, t') = -i \langle T_C \{ a_\nu(t^\alpha) a_\nu^\dagger(t'^\beta) \} \rangle$  ( $\nu$  means quantum numbers of edge or bulk state) and photons  $D_{\mathbf{q}, \lambda}^{\alpha\beta}(t, t') = -i \langle T_C \{ c_{\mathbf{q}, \lambda}(t^\alpha) c_{\mathbf{q}, \lambda}^\dagger(t'^\beta) \} \rangle$  ( $\alpha, \beta = \pm$ ). Following standard procedure<sup>22</sup> we obtain a kinetic equation for Green function that determines population distribution of edge state ( $G_e^<(t, t) = G_e^{-+}(t, t)$ ):

$$i \frac{\partial}{\partial t} G_e^<(t, t) = \int_{-\infty}^{+\infty} \Sigma_{ee}^R(t, t_1) G_e^<(t_1, t) dt_1 + \int_{-\infty}^{+\infty} \Sigma_{ee}^<(t, t_1) G_e^A(t_1, t) dt_1 - \int_{-\infty}^{+\infty} G_e^R(t, t_1) \Sigma_{ee}^<(t_1, t) dt_1 - \int_{-\infty}^{+\infty} G_e^<(t, t_1) \Sigma_{ee}^A(t_1, t), \quad (\text{A5})$$

where  $G^R = G^{--} - G^{-+}$ ,  $G^A = G^{--} - G^{+-}$ . In the Eq. (A5) we calculate self-energies in the second order in perturbation (A3):

$$\begin{aligned} \Sigma_{ee}^R(t_1, t_2) &= \Sigma_{ee}^{--}(t_1, t_2) + \Sigma_{ee}^{-+}(t_1, t_2) = \\ & i \sum_{\mathbf{p}, \mathbf{q}, \lambda} \left| V_{\varepsilon_v, \varepsilon_e}^{(\lambda, \tau)}(\mathbf{q}) \right|^2 \left[ D_{0_{\mathbf{q}, \lambda}}^{--}(t_1, t_2) G_{0_{\mathbf{p}, \varepsilon_v}}^{--}(t_1, t_2) - \right. \\ & \left. D_{0_{\mathbf{q}, \lambda}}^{-+}(t_1, t_2) G_{0_{\mathbf{p}, \varepsilon_v}}^{-+}(t_1, t_2) \right] = \\ & -i\theta(t_1 - t_2) \times \\ & \sum_{\mathbf{p}, \mathbf{q}, \lambda} \left| V_{\varepsilon_v, \varepsilon_e}^{(\lambda, \tau)}(\mathbf{q}) \right|^2 [n_0 \delta_{\lambda, +} \delta_{\mathbf{q}, \mathbf{q}_0} + (1 - f_v)] e^{-i(\varepsilon_v + \omega)(t_1 - t_2)}, \\ \Sigma_{ee}^<(t_1, t_2) &= -\Sigma_{ee}^{-+}(t_1, t_2) = \\ & i \sum_{\mathbf{p}} \left| V_{\varepsilon_v, \varepsilon_e}^{(+, \tau)}(\mathbf{q}_0) \right|^2 n_0 f_v e^{-i(\varepsilon_v + \omega_0)(t_1 - t_2)}, \\ \Sigma_{ee}^R(t_1, t_2) &= [\Sigma_{ee}^A(t_2, t_1)]^*. \quad (\text{A6}) \end{aligned}$$

where the terms with wave vector  $\mathbf{q}_0 = (0, 0, -q_0)$  describe transitions induced by illuminated light with frequency  $\omega_0 = cq_0$  and clockwise polarisation,  $n_0 = -iD_{0_{\mathbf{q}_0, +}}^{-+}(t, t)$  is the number of the illuminated light quanta, the term proportional to  $1 - f_v$  (where  $f_v = -iG_{0_{\mathbf{p}, \varepsilon_v}}^{-+}(t, t)$  is Fermi-Dirac distribution function in valence band) concerns with spontaneous recombination processes. After substitution of Green functions of zero approximation  $G_e^A(t_1, t_2) = [G_e^R(t_2, t_1)]^* = i\theta(t_2 - t_1) e^{i\varepsilon_e(t_2 - t_1)}$ ,  $G_e^<(t_1, t_2) = if_e(t) e^{i\varepsilon_e(t_2 - t_1)}$  in Eq. (A5) and accounting for only contributions from poles at integration over time we arrive to a kinetic equation similar to that used in the main text (13):

$$\frac{\partial f_e}{\partial t} = \frac{I\Omega}{c\hbar\omega_0} \frac{2\pi}{\hbar} \sum_{\mathbf{p}} \left| V_{\varepsilon_v, \varepsilon_e}^{(+, \tau)}(\mathbf{q}_0) \right|^2 [f_v - f_e] \delta(\varepsilon_v - \varepsilon_e + \hbar\omega_0) - f_e \frac{2\pi}{\hbar} \sum_{\mathbf{p}, \mathbf{q}, \lambda = \pm} \left| V_{\varepsilon_v, \varepsilon_e}^{(\lambda, \tau)}(\mathbf{q}) \right|^2 [1 - f_v] \delta(\varepsilon_v - \varepsilon_e + \hbar\omega) - \frac{f_e - f_{eq}}{\tau_R}, \quad (\text{A7})$$

where we add the term with phenomenological relaxation time  $\tau_R$  as in the main text,  $n_0 = I\Omega/c\hbar\omega_0$ .

## Appendix B: General relation for quasi Fermi-levels

In the section we will obtain a general relation for quasi Fermi-levels of DFs in valence and edge bands under illu-

mination of the light. Introducing the density of valence band states with definite momentum (15) we rewrite Eq. (A7) in the following form:

$$\begin{aligned} & \frac{I}{I_0} \left[ \delta_{\tau,1} + \delta_{\tau,-1} \left( \frac{\hbar v \kappa_e + \tau v p_e}{2\tilde{m}a} \right)^2 \right] [f_v(\varepsilon - \hbar\omega_0) - f_e(\varepsilon)] \frac{\sqrt{\varepsilon_t - \frac{v^2 p_e^2}{2\tilde{m}} - \varepsilon + \hbar\omega_0}}{\left[ \frac{(\hbar v \kappa_e)^2}{2\tilde{m}} + \varepsilon_t - \frac{v^2 p_e^2}{2\tilde{m}} - \varepsilon + \hbar\omega_0 \right]^2} - \\ & \frac{f_e(\varepsilon)}{12\pi^2 (\hbar\omega_0)^2} \left[ 1 + \left( \frac{\hbar v \kappa_e + \tau v p_e}{2\tilde{m}a} \right)^2 \right] \int_0^{+\infty} d(\hbar\omega) \frac{\hbar\omega [1 - f_v(\varepsilon - \hbar\omega)] \sqrt{\varepsilon_t - \frac{v^2 p_e^2}{2\tilde{m}} - \varepsilon + \hbar\omega}}{\left[ \frac{(\hbar v \kappa_e)^2}{2\tilde{m}} + \varepsilon_t - \frac{v^2 p_e^2}{2\tilde{m}} - \varepsilon + \hbar\omega \right]^2} - \\ & \frac{(1+a^2)n_r^2 c^3 \sqrt{2\tilde{m}}}{4a^2 \pi \tau_R (ve)^2 \omega_0^2 \hbar v \kappa_e} [f_e(\varepsilon) - f_{eq}(\varepsilon)] = 0 \end{aligned} \quad (\text{B1})$$

To proceed further analytically, we consider low temperature limit ( $T \ll \min(\mu_{e,\tau}, \mu_{v,\tau})$ ) to treat Fermi-functions

as step-like ones. Then we integrate the above equation over energy and arrive a final relation between quasi Fermi-levels  $\mu_{e,\tau}, \mu_{v,\tau}$ :

$$\begin{aligned} & \frac{I}{I_0} \left[ \delta_{\tau,1} + \delta_{\tau,-1} \left( \frac{\hbar v \kappa_F}{2\tilde{m}a} \right)^2 \right] \left\{ \arctan \left[ \frac{\kappa_F (k_{y0}(\mu_{e,\tau} - \hbar\omega_0) - k_{y0}(\mu_{v,\tau}))}{\kappa_F^2 + k_{y0}(\mu_{e,\tau} - \hbar\omega_0) k_{y0}(\mu_{v,\tau})} \right] + \frac{\kappa_F k_{y0}(\mu_{v,\tau})}{\kappa_F^2 + k_{y0}^2(\mu_{v,\tau})} \right\} - \\ & \theta(\mu_{e,\tau} - \varepsilon^*) \frac{\kappa_F \left[ 1 + \left( \frac{\hbar v \kappa_0}{2\tilde{m}a} \right)^2 \right]}{12\pi^2 \kappa_0 (\hbar\omega_0)^2} \left\{ 6(\hbar v)^2 \kappa_0 k_{y0}(\mu_{v,\tau}) \frac{\mu_{e,\tau} - \varepsilon^*}{2\tilde{m}} - \frac{\kappa_F k_{y0}(\mu_{v,\tau})}{\kappa_F^2 + k_{y0}^2(\mu_{v,\tau})} \left[ (\mu_{e,\tau} - \mu_{v,\tau})^2 - (\varepsilon^* - \mu_{v,\tau})^2 \right] + \right. \\ & \left. \arctan \left( \frac{k_{y0}(\mu_{v,\tau})}{\kappa_0} \right) \left[ \left( \mu_{e,\tau} - \varepsilon_t - 3 \frac{(\hbar v \kappa_0)^2}{2\tilde{m}} \right)^2 - \left( \varepsilon^* - \varepsilon_t - 3 \frac{(\hbar v \kappa_0)^2}{2\tilde{m}} \right)^2 \right] \right\} - \frac{(1+a^2)n_r^2 c^3}{4a^2 \pi \tau_R \omega_0^2 (ve)^2} [\mu_{e,\tau} - \varepsilon_F] = 0, \end{aligned} \quad (\text{B2})$$

where  $k_{y0}(\varepsilon) = k_y(\varepsilon, 0)$ ,  $\kappa_F = \kappa(\varepsilon_F)$ ,  $\kappa_0 = \kappa(\varepsilon_e(0))$ . At integration we neglected by dependence of ES decay length and terms proportional to  $vp_e/2\tilde{m}$  on the energy.

In the limit  $\rho_e/\rho_v \ll 1$  we can neglect by the terms proportional to  $k_{y0}(\mu_{v,\tau})$  in Eq.(B2), which leads us to the Eq.(18) used in the main text of the manuscript.

\* vova.enaldiev@gmail.com

<sup>1</sup> Z. Sun, A. Martinez, and F. Wang, Nature Photonics **10**,

- 227 (2016).
- <sup>2</sup> A. Pospischil, M. M. Furchi, and T. Mueller, *Nature nanotechnology* **9**, 257 (2014).
  - <sup>3</sup> A. Kormányos, G. Burkard, M. Gmitra, J. Fabian, V. Zólyomi, N. D. Drummond, and V. Fal'ko, *2D Materials* **2** (2015).
  - <sup>4</sup> G. Moody, C. K. Dass, K. Hao, C.-H. Chen, L.-J. Li, A. Singh, K. Tran, G. Clark, X. Xu, G. Berghäuser, *et al.*, *Nature communications* **6**, 8315 (2015).
  - <sup>5</sup> X. Yin, Z. Ye, D. A. Chenet, Y. Ye, K. O'Brien, J. C. Hone, and X. Zhang, *Science* **344**, 488 (2014).
  - <sup>6</sup> C. Zhang, A. Johnson, C.-L. Hsu, L.-J. Li, and C.-K. Shih, *Nano letters* **14**, 2443 (2014).
  - <sup>7</sup> M. Bollinger, J. Lauritsen, K. W. Jacobsen, J. K. Nørskov, S. Helveg, and F. Besenbacher, *Physical review letters* **87**, 196803 (2001).
  - <sup>8</sup> D. Wu, X. Li, L. Luan, X. Wu, W. Li, M. N. Yogeesh, R. Ghosh, Z. Chu, D. Akinwande, Q. Niu, *et al.*, *Proceedings of the National Academy of Sciences*, 201605982 (2016).
  - <sup>9</sup> M. Bollinger, K. W. Jacobsen, and J. K. Nørskov, *Physical Review B* **67**, 085410 (2003).
  - <sup>10</sup> C. Ataca, H. Sahin, E. Akturk, and S. Ciraci, *The Journal of Physical Chemistry C* **115**, 3934 (2011).
  - <sup>11</sup> E. Erdogan, I. Popov, A. Enyashin, and G. Seifert, *The European Physical Journal B-Condensed Matter and Complex Systems* **85**, 1 (2012).
  - <sup>12</sup> A. Vojvodic, B. Hinnemann, and J. K. Nørskov, *Physical Review B* **80**, 125416 (2009).
  - <sup>13</sup> Y. Li, Z. Zhou, S. Zhang, and Z. Chen, *Journal of the American Chemical Society* **130**, 16739 (2008).
  - <sup>14</sup> F. Khoeyi, K. Shakouri, and F. Peeters, *Physical Review B* **94**, 125412 (2016).
  - <sup>15</sup> H. Rostami, R. Asgari, and F. Guinea, *Journal of Physics: Condensed Matter* **28**, 495001 (2016).
  - <sup>16</sup> C. G. Péterfalvi, A. Kormányos, and G. Burkard, *Physical Review B* **92**, 245443 (2015).
  - <sup>17</sup> V. A. Volkov and V. V. Enaldiev, *Journal of Experimental and Theoretical Physics* **122**, 608 (2016).
  - <sup>18</sup> C. Segarra, J. Planelles, and S. Ulloa, *Physical Review B* **93**, 085312 (2016).
  - <sup>19</sup> M. Trushin, E. J. Kelleher, and T. Hasan, *Physical Review B* **94**, 155301 (2016).
  - <sup>20</sup> K. F. Mak, K. L. McGill, J. Park, and P. L. McEuen, *Science* **344**, 1489 (2014).
  - <sup>21</sup> D. Xiao, G.-B. Liu, W. Feng, X. Xu, and W. Yao, *Physical Review Letters* **108**, 196802 (2012).
  - <sup>22</sup> P. I. Arseev, *Physics-Uspekhi* **58**, 1159 (2015).
  - <sup>23</sup> H. Shi, R. Yan, S. Bertolazzi, J. Brivio, B. Gao, A. Kis, D. Jena, H. G. Xing, and L. Huang, *ACS nano* **7**, 1072 (2013).
  - <sup>24</sup> R. Wang, B. A. Ruzicka, N. Kumar, M. Z. Bellus, H.-Y. Chiu, and H. Zhao, *Physical Review B* **86**, 045406 (2012).